An environmentally friendly water-activated manganese dioxide battery

K. VUORILEHTO

*Helsinki University of Technology, Laboratory of Corrosion and Material Chemistry, Vuorimiehentie 2, FIN-02150
Espoo, Finland*
(Fax: +358 9 4512798)

Abstract

In this work an environmentally friendly water-activated battery was developed and investigated. The anode material was a magnesium alloy; the cathode consisted of manganese dioxide, potassium chloride and graphite. Battery characteristics were tested at room temperature and additionally in an atmospheric simulation chamber because water-activated batteries are mostly used in meteorological radiosondes. Voltage losses inside the battery were measured using a miniaturized reference electrode, and heat evolution of the battery was studied calorimetrically. The main source of voltage losses and heat was found to be the magnesium anode. Compared to the traditional Mg/CuCl batteries, there was little difference in voltage and capacity, but a significant difference in the environmental impact, as the Mg/MnO_2 battery does not contain any heavy metal salts.

1. Introduction

Water-activated batteries are reserve batteries, to which water is added prior to use. This makes it possible to use very reactive materials without the problem of self-discharge. The water forms the electrolyte with ions produced in electrode reactions or released from a soluble salt.

Water-activated batteries are used as power sources in radiosondes, air rescue equipment, life jackets and lifeboats, emergency rockets, missiles, torpedoes and underwater research devices. The batteries in question have to withstand long periods of storage without self-discharge, and they are exploited under difficult temperature conditions, especially at very low temperatures. Almost all water-activated batteries are applied in nature, and most of them remain there after use, so their environmental impact cannot be neglected [1].

The magnesium/copper(I) chloride battery is the usual and traditional type of water-activated battery [1–3]. Its drawback is the solubility of copper ions, which cause on the one hand corrosion of the magnesium anode and overheating, and on the other hand environmental hazards. The aim of this work was to study manganese dioxide as an environmentally friendly alternative to CuCl, to determine the differences between the batteries and to develop an optimized MnO_2 battery. MnO_2 was chosen for the studies because it is known as a non-toxic chemical [4] and a feasible cathode material [5, 6].

2. Experimental details

2.1. *Construction of the batteries*

The battery studied is shown in Figure 1. The anode was a magnesium alloy AZ-31 with 3% (by mass) aluminium and 1% zinc, manufactured by Spectrulite Consortium, USA. The reactive cathode material was electrochemically deposited manganese dioxide MnO_2, manufactured by Tosoh Hellas, Greece. The amount of reactive material was sufficient for about six hours' use. In addition the cathodes contained 11–21% (by mass) soluble salt (KCl, NaCl, LiCl or $MgCl_2$) as an ionic conductor, 7% expanded graphite (Timcal, Switzerland) as an electronic conductor and 2% polytetrafluoroethene (Dyneon, Germany) as a binder. In some experiments, 0.5% magnesium hydroxide, $Mg(OH)_2$, was added to the cathode mix to make the electrolyte more alkaline. Cathode mixes were prepared in quantities of 200 g and the materials were ground for 30 seconds in an Ika M20 Universal Mill. The powder was compressed into cathode pellets using a pressure of about 180 MPa. One cathode pellet had a geometric surface area of (2.5×5.8) cm^2 (i.e., 14.5 cm^2) and was about 0.13 cm thick.

The anode and cathode of each cell were separated by a layer of polyester wool, which was able to absorb the activation water. One battery consisted of twelve such cells connected in series by an inert carbon foil. Short circuit currents between the cells were eliminated by
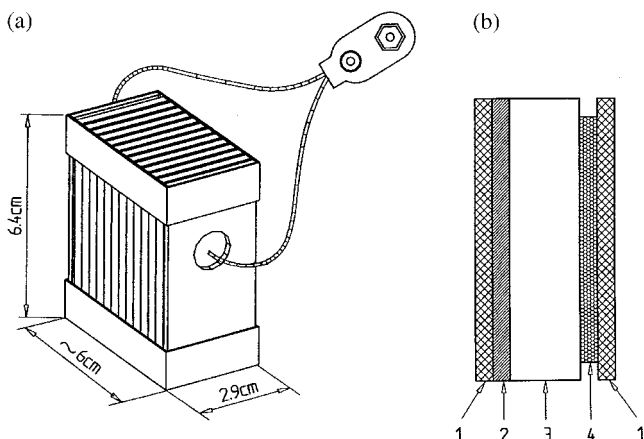
(a)

(b)

Fig. 1. (a) The battery studied comprising 12 cells with dry mass 120 g. (b) Section through the cell: (1) carbon foil, (2) magnesium anode, (3) polyester wool and (4) manganese dioxide cathode.

putting adhesive tape on the edge of the polyester wool. Additionally, the sides of the battery were covered with adhesive tape. The bottom of the battery was waxed. The finished battery was packed in hermetic foil to avoid self-discharge.

Prior to use the battery had to be activated by immersing it in tap water for three minutes. The polyester wool was able to absorb approximately 48 g of water (4 g per cell). The start-up electrolyte was formed from the water and the soluble salt that dissolved from the cathode.

2.2. *Battery reactions*

The current-producing reaction of the manganese dioxide cathode is the same as in conventional alkaline batteries at pH 14 [1]:

$$MnO_2 + H_2O + e^- \rightarrow MnOOH + OH^-$$
$$E^\circ = +0.1 \, V \text{ vs SHE} \tag{1}$$
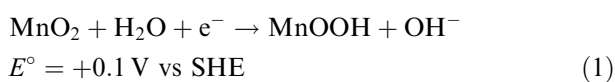
The MnOOH product forms a solid solution with the MnO_2 reactant, giving rise to a continuously decreasing cathode potential. According to the manufacturer, the alkaline potential of fresh MnO_2 powder is $+0.255$ V, whereas the potential $+0.1$ V given in Equation 1 was estimated for the half-discharged MnO_2, using Pourbaix diagrams [7]. These, like most chemical reference works, do not take manganese(III) as MnOOH but as Mn_2O_3. Therefore MnOOH was assumed to be equivalent to $\frac{1}{2}(Mn_2O_3 + H_2O)$.

The anode reaction of the battery is [1, 2]

$$Mg \rightarrow Mg^{2+} + 2e^- \quad E^\circ = -2.360 \, V \text{ vs SHE} \tag{2}$$
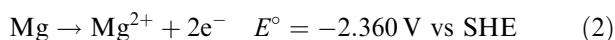
In an aqueous solution a passivating hydroxide layer is formed on the magnesium surface, and therefore the electrode potential of magnesium is 0.6 to 1.1 V more positive than the theoretical potential [2].

Combining Equations 1 and 2, the total cell reaction is

$$Mg + 2 MnO_2 + 2 H_2O \rightarrow 2 MnOOH + Mg^{2+} + 2 OH^-$$
$$\Delta H = -558 \, kJ \, mol^{-1} \, [8] \tag{3}$$
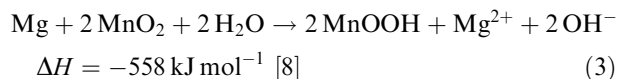
The magnesium and hydroxide ions are produced at opposite sides of the cell. As they diffuse into the separator, they precipitate:

$$Mg^{2+} + 2 OH^- \rightarrow Mg(OH)_2 \quad \Delta H = +2 \, kJ \, mol^{-1} \, [8] \tag{4}$$
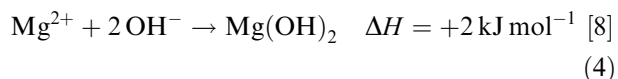
Using Equations 1, 2 and 3 the theoretical voltage of a Mg/MnO_2 cell can be calculated:

$$U^\circ = +0.1 \, V - -2.360 \, V = 2.46 \, V$$
(29.5 V for 12 cells)

For comparison, the theoretical voltage of a sulfur-containing Mg/CuCl cell is [9]:

$$U^\circ = +0.531 \, V - -2.360 \, V = 2.89 \, V$$
(34.7 V for 12 cells)

Magnesium, being an electropositive metal, oxidises, i.e. corrodes, very easily. In addition to the desired electrode reaction (Equation 2) a hydrogen-producing corrosion reaction takes place at the anode [1, 2]:

$$Mg + 2 H_2O \rightarrow Mg(OH)_2 + H_2$$
$$\Delta H = -353 \, kJ \, mol^{-1} \, [8] \tag{5}$$
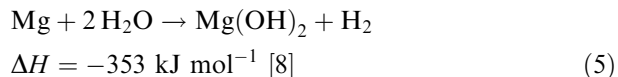
This corrosion reaction is strongly exothermic. In cold conditions during radiosonde soundings the corrosion of the magnesium anode produces the heat needed to keep the battery temperature above 0 °C. However, when corrosion catalysts, such as copper, iron, chloride or bromide, are present, corrosion may generate too much heat. As a consequence the water evaporates, the electrolyte diminishes and the battery voltage drops. Copper and iron cause galvanic corrosion, whereas the aggressive ions, chloride and bromide, cause pitting corrosion [10].

2.3. *Tests at room temperature*

Room temperature experiments required active heat transfer because of the extensive heat production of the battery. Therefore the test battery, contained in a small plastic bag, was placed in a water filled, thermally insulated Dewar flask (22–23 °C). During battery discharge, the heat was transferred from the battery through the plastic bag to the water. Due to its high heat capacity, the water warmed up only a few degrees. In most experiments the discharge current was 150 mA (10 mA cm^{-2}), and discharge was continued until battery voltage dropped below 10 V. As the theoretical voltage is 29.5 V, it was estimated that practically all

available energy was depleted at 10 V. The battery voltage and the temperature rise of the water were measured as a function of time. Heat energy and heat evolution power were determined using the heat capacity of water.

2.4. *Simulations in the atmospheric chamber*

Radiosondes are the main use of water-activated batteries. A radiosonde is a measuring device used for meteorological research in the upper atmosphere. During a sounding the radiosonde is raised to a height of $20 \sim 40$ km by a weather balloon. Simultaneously it measures and transmits information on temperature, pressure and air humidity. The conditions during radiosonde soundings in the upper atmosphere are extreme: the temperature decreases to approximately $-60 \sim -90$ °C, and the pressure falls to approximately 10 mbar.

To test battery performance in radiosonde use, battery characteristics were studied in an atmospheric simulation chamber (Weiss, Germany), in which temperature and pressure were adjusted to values similar to those in normal radiosonde soundings. The temperature and pressure profiles during a simulation are given in Table 1. The air flow during radiosonde soundings was simulated by ventilation, and a computer controlled the temperature and pressure in the chamber and recorded their values. The duration of the simulation program was 150 min. During the first 30 min of discharge, 30 min being the assumed period needed for ground preparation of a sounding, the temperature was 25 °C and the pressure was 1015 mbar. The batteries were discharged using a direct current of 150 mA and they were required to give at least a cut-off voltage of 15 V, which are typical values required by a modern radiosonde. The battery voltage was measured during simulation and presented as a function of time. The time, in which the battery voltage stayed above the cut-off voltage, was determined.

Table 1. Pressure and temperature profiles during an atmospheric simulation. An operation time of 135 min is normally required for radiosondes (including the ground preparation)

Time /min	p /mbar	T /°C	Height /km
0–30	1015	+25	0
35	843	+10	1.5
45	572	−15	4.6
55	377	−34	7.6
65	239	−55	10.7
75	148	−60	13.7
85	92	−60	16.8
95	57	−60	19.8
105	35	−60	22.9
115	22	−60	25.9
125	15	−60	28.9
135	10	−60	31.7
150	7.5	−60	33.4

2.5. In situ *measurements*

Some room temperature tests and atmospheric simulations were interrupted at 135 min in order to make *in situ* measurements. (An operation time of 135 min is required for radiosonde use.) A miniaturized Ag|AgCl reference electrode (Kurt Schwabe Institut, Germany) was placed inside the battery on the surface of individual electrodes and the electrode potentials were measured. By measuring the potential difference over the polyester separator, the *IR* drop in the separator could be estimated. The *in situ* experiments provided data about the voltage losses at the individual electrodes and in the separator.

3. Results and discussion

3.1. *Various chlorides in the cathode*

Voltage curves obtained in discharge tests at room temperature for batteries with various chloride salts are shown in Figure 2. The aim of the chloride salts in the cathodes was to make the aqueous electrolyte ionically conductive. Previous research [11] had shown that chlorides are preferable salts, as chloride ions depassivate the magnesium effectively.

As can be seen, KCl produced the best result, although NaCl performed almost as well. Cathodes with LiCl and $MgCl_2$ additions worked poorly. The reason for this striking difference lies in the conductivity. Inside the cathode pores, highly conductive concentrated KOH or NaOH solutions form due to Reaction 1, when using KCl or NaCl respectively. Similar concentrated solutions of LiOH or $Mg(OH)_2$ cannot form, as they are far less soluble [12].

Voltage curves for batteries with various amounts of KCl are shown in Figure 3. It can be seen that a smaller
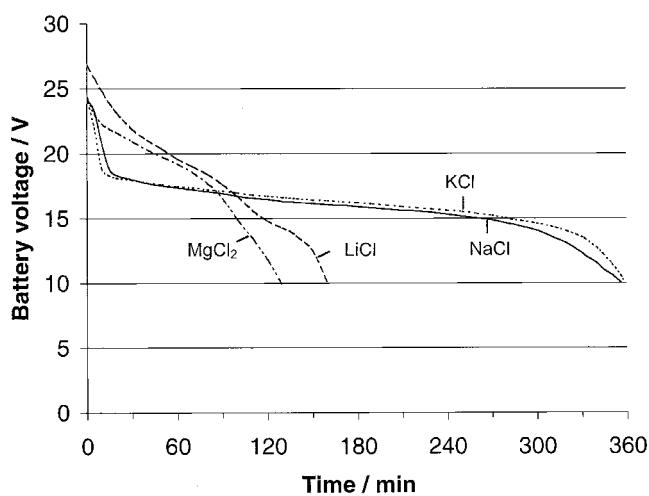
Fig. 2. Voltage curves at room temperature and normal pressure for various chloride salts: (······) 11% KCl, (——) 11% NaCl, (− − −) 11% LiCl and (–··–) 21% $MgCl_2$. Magnesium chloride ($MgCl_2.6\ H_2O$) additions were larger due to the mass of the crystal water. Discharge current 150 mA (10 mA cm^{-2}).
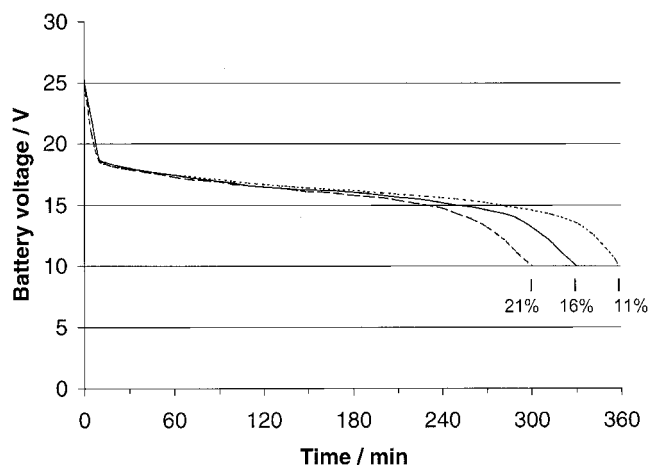
Fig. 3. Voltage curves at room temperature and normal pressure for various amounts of potassium chloride: ($\cdots\cdots$) 11% KCl, (——) 16% KCl, and (– – –) 21% KCl. Discharge current 150 mA (10 mA cm^{-2}).

amount of KCl, and thus a larger amount of MnO$_2$, increases the capacity. This is logical, as MnO$_2$ is the capacity limiting factor of the battery. However, if the amount of KCl is too small, the *IR* drop in the electrolyte is very high. A battery with 6% of KCl showed inferior performance in preliminary tests and was not studied further.

3.2. *Influence of the atmosphere*

The results of the tests in the atmospheric chamber are listed in Table 2, together with results obtained for the same batteries at room temperature. The batteries worked for a much shorter time in the atmospheric chamber than at room temperature (except for the MgCl$_2$ battery that worked badly in both cases). In addition, all batteries with KCl or NaCl worked for 135 ± 4 min, although the differences at room temperature were significant. The real capacity of the battery seemed to have little influence on the battery performance in the atmospheric chamber.

The reason for these phenomena is the air pressure. At low pressures the boiling point of water decreases rapidly; at 135 min, the pressure is 10 mbar and the boiling point only 7 °C. A battery cannot be warmer than the boiling point of its electrolyte, and the

Table 2. Results of the discharge tests at room temperature and in the atmospheric chamber

Salt	Duration at room temperature /min	Duration in the atmospheric chamber /min
11% KCl	279	139
16% KCl	251	136
21% KCl	230	135
11% NaCl	261	132
11% LiCl	116	103
21% MgCl$_2 \cdot$ 6H$_2$O	98	102

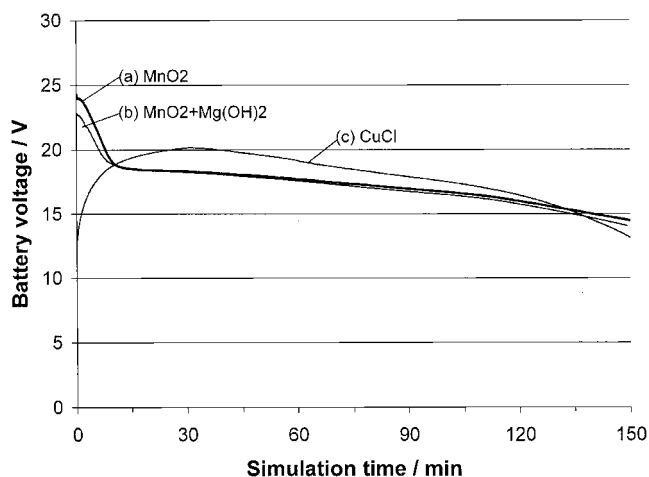Discharge current 150 mA (measured to a cut-off voltage of 15 V).

Fig. 4. Voltage curves in the atmospheric simulation chamber for (a) a MnO$_2$ battery (80% MnO$_2$ + 11% KCl + 7%C + 2% PTFE), (b) a MnO$_2$ battery (79.5% MnO$_2$ + 11% KCl + 7%C + 2% PTFE + 0.5% Mg(OH)$_2$), (c) a CuCl battery (59% CuCl + 30%S + 10% C + 1% Mg-stearate). The discharge current was 150 mA (10 mA cm^{-2}).

temperature range, in which the battery neither boils nor congeals, becomes very narrow. Part of the electrolyte is lost by boiling and simultaneously the low temperature decelerates the cell reactions. The fast growing *IR* drop of the diminishing electrolyte, combined with the overpotentials of the cell reactions, reduces the battery voltage to below 15 V.

The discharge curve of the 11% KCl battery, obtained in atmospheric simulation, can be seen in Figure 4, curve (a).

3.3. *Mg(OH)$_2$ and the voltage peak*

In each discharge curve the initial high voltage rapidly decreases during the first minutes, as seen in Figures 2–4. The voltage peak is caused by the neutral pH of the activation water, which makes the potential of cathode Reaction 1 very positive. The voltage decreases as this same reaction produces OH$^-$ ions which increase the pH value and decrease the cathode potential. The drop continues until the pH inside the cathode pores settles. With KCl and NaCl this happens at pH 14–15.

An attempt was made to eliminate the voltage peak by adding 0.5% magnesium hydroxide, Mg(OH)$_2$, to the cathode mix. By this means the electrolyte inside the cathode became alkaline (pH 10) at the very beginning.

The result can be seen in Figure 4, curve (b). The peak was cut, but only partly, as pH still increased from 10 to 14.5. An addition of KOH or NaOH would increase pH more than an addition of Mg(OH)$_2$, and cut the peak more efficiently. Unfortunately, a very high initial pH passivates the magnesium anode, as seen in preliminary experiments.

3.4. *Voltage losses*

The actual voltage of the Mg/MnO$_2$ battery remains significantly lower than the theoretical voltage of

Table 3. Comparison of battery voltages at room temperature and in the atmospheric chamber after 135 min of 150 mA discharge

	Room temperature	Atmospheric chamber	Difference
Theoretical voltage/V	29.5	29.5	0.0
Cathode overpotential η_C/V	−0.2	−1.0	0.8
Loss at the Mg-anode η_A/V	−12.3	−12.3	0.0
IR drop (separator)/V	−0.4	−1.0	0.6
IR drop (carbon foil)/V	−0.2	−0.2	0.0
Resulting voltage/V	16.4	15.0	1.4

To measure the electrode potentials in the atmospheric chamber, normal pressure had to be restored. This may have caused experimental errors not exceeding 0.2 V.

29.5 V. In addition there is a clear difference between the voltages at room temperature and in the atmospheric chamber. Therefore the sources of the voltage losses were investigated.

The actual battery voltage is always lower than the theoretical, depending on reaction kinetics and cell resistance:

$$U = E_t^C - E_t^A - |\eta_C| - |\eta_A| - IR_{cell} \quad (6)$$

where E_t^C and E_t^A are the thermodynamic potentials for the cathodic and anodic reactions respectively, η_C and η_A are the overpotentials of the electrode reactions, I is the current and R_{cell} is the cell resistance.

A comparison of the voltages at room temperature and in the atmospheric chamber is presented in Table 3. Batteries with 11% KCl were used and the voltages were measured after 135 min of discharge. The overpotential η_C at the manganese dioxide cathode was estimated with a miniaturized reference electrode by subtracting the measured cathode potential from the theoretical potential of Reaction 1. The overpotential η_A at the magnesium anode was estimated by subtracting the measured anode potential from the theoretical potential of Reaction 2. This was not a pure overpotential, but merely a voltage loss caused by the hydroxide layer and the hydrogen evolution; this voltage loss did not depend on the environmental conditions. The IR drop in the separator was estimated by comparing electrode potentials measured at both sides of the separator. In addition to the IR drop in the separator, there was some IR drop in the electric contacts, mainly on the carbon foil. This was measured with an ohmmeter.

It can be estimated that over 90% of the actual room temperature voltage loss is due to the irreversibility of the magnesium anode. Low temperature had no effect on this loss, possibly because corrosion Reaction 5 keeps the magnesium surface warm.

The difference between room temperature and atmospheric chamber voltages originates from the MnO_2 cathode and the separator. Low temperature in the atmospheric chamber causes high activation and diffusion overpotentials at the cathode, and evaporation of the electrolyte causes a high IR loss in the separator.

3.5. *Heat evolution*

In room temperature discharge tests, the heat evolution power of the Mg/MnO_2 battery was measured to be about 4.9 W. As this is significantly more than the average electric power of the battery, 2.6 W, an attempt was made to discover the origin of the heat.

Heat can be produced by the cell reaction of the battery and by a possible side reaction. These sources of heat evolution power (Q_{hep}) can be calculated from Equation 7:

$$Q_{hep} = I_{cell} \times (-\Delta H_{cell}/zF - U_{cell}) + I_{side} \times (-\Delta H_{side}/zF) \quad (7)$$

where I is the current, U is the voltage, ΔH is the enthalpy change, z is the number of electrons (2) and F is the faradaic constant (96 500 C mol^{-1}). $-\Delta H/zF$ values are used instead of $U°$ values as the latter include entropy effects.

For a Mg/MnO_2 battery the ΔH of the cell reaction was calculated by combining Reactions 3 and 4, −558 kJ mol^{-1} + 2 kJ mol^{-1} = −556 kJ mol^{-1}. The average cell voltage during the calorimetric experiments was 17.5 V/12=1.46 V. The only significant side reaction was corrosion of magnesium, Reaction 5. The current of this side reaction, I_{side}, was estimated from the current efficiency (0.60), which had been measured previously in connection with corrosion experiments for magnesium [13]. The ΔH of this side reaction is −353 kJ mol^{-1}. The calculation using Equation 7 gives the following result for the average heat evolution power ($\bar{Q}_{hep}$) of the Mg/MnO$_2$ battery with 12 cells:

$$\begin{aligned} \bar{Q}_{hep} &= 12 \times 0.150\,A \times (2.88\,V - 1.46\,V) \\ &\quad + 12 \times (0.150\,A/0.60 - 0.150\,A) \times 1.83\,V \\ &= 2.56\,W + 2.20\,W = 4.76\,W \end{aligned}$$

The experimental value of 4.9 W is in good agreement with this theoretically calculated one. It can be seen that 2.56 W (54%) of the heat evolution originated from the cell reaction. The main cause of this heat was the magnesium overpotential. From Table 3, its magnitude can be calculated to be 0.15 A × 12.3 V = 1.85 W (=39%). As 2.20 W (46%) of the heat evolution originated from the magnesium corrosion side reaction, it can be concluded that magnesium is the source of almost all (85%) of the heat.

3.6. *Energy density and power density*

The energy density of the Mg/MnO_2 battery at room temperature is 87 Wh kg^{-1} and the power density is 15 W kg^{-1} when using a discharge current of 150 mA (calculated from the data in Figure 3, 11% KCl). These values are comparable to those of fresh alkaline Zn/MnO$_2$ batteries at same discharge rate, 70 Wh kg^{-1} and 20 W kg^{-1} [14].
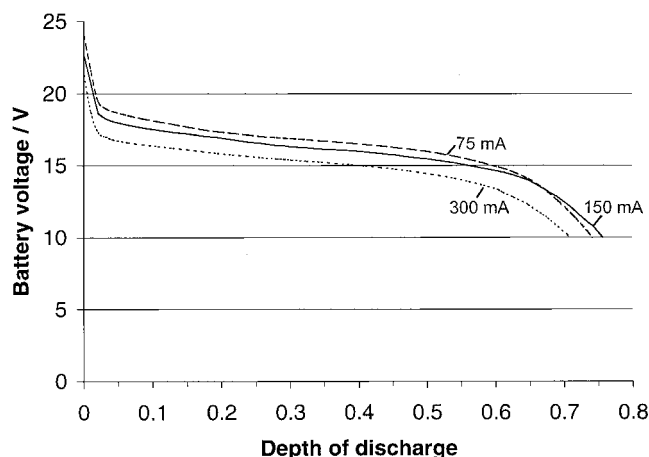
Fig. 5. Voltage curves at room temperature and normal pressure for various discharge currents: $(---)$ 75 mA (5 mA cm^{-2}), (——) 150 mA (10 mA cm^{-2}) and $(\cdots\cdots)$ 300 mA (20 mA cm^{-2}). The cathodes consisted of 79.5% MnO$_2$ + 11% KCl + 7%C + 2% PTFE + 0.5% Mg(OH)$_2$. Depth of discharge is the proportion of MnO$_2$ that has been consumed for current production.

Although the Mg/MnO$_2$ battery was designed for a discharge current of 150 mA, it is of interest how it works when other discharge currents are applied. In Figure 5, voltage curves for three different discharge currents are compared. To facilitate comparison, depth of discharge is used in this figure instead of discharge time. Changing the discharge current by a factor of two makes little impact on voltage and capacity. This is explained by the low *IR* drops at room temperature, seen in Table 3. Another interesting feature is the lower capacity at 75 mA compared to the capacity at 150 mA. This was caused by the corrosion side reaction that became significant during the 12 h of 75 mA discharge. Energy and power densities for different discharge currents are listed in Table 4.

3.7. *Comparison of Mg/MnO$_2$ and Mg/CuCl batteries*

Discharge curves of Mg/MnO$_2$ and Mg/CuCl batteries, obtained in atmospheric simulations, can be seen in Figure 4. Although performance in atmospheric simulations is compared here, the same phenomena can be observed in room temperature tests.

Table 4. Energy and power densities for various discharge currents at room temperature

Discharge current / mA	Energy density /Wh kg^{-1}	Power density /W kg^{-1}
75	90	8
150	87	15
300	75	27

Results calculated from Figure 5 to 10 V. Wet mass of batteries 0.165 kg.

Both batteries stay above the cut-off voltage of 15 V for about 135 min. However, the first parts of the discharge curves differ significantly. The Mg/MnO$_2$ battery starts immediately without any delay effect. This is due to the large amount of potassium chloride that dissolves during activation, making the aqueous electrolyte ionically conductive and breaking the passive layer of the magnesium anode. In the Mg/CuCl battery, the electrolyte consists mainly of magnesium chloride which is produced in cell reactions during discharge. Therefore, there is little MgCl$_2$ at the beginning of discharge, resulting in a long delay time.

The average voltage of the Mg/MnO$_2$ battery is slightly lower than that of the Mg/CuCl battery, as expected from the lower theoretical voltage (29.5 vs 34.7 V). At the end of discharge, this is compensated by a slower voltage decrease of the Mg/MnO$_2$ battery. The reason for this more stable voltage is the lack of soluble copper ions which cause excessive corrosion of magnesium and overheating in the Mg/CuCl battery.

The main difference between the batteries is the ecological impact of the soluble copper liberated during activation and use of the Mg/CuCl batteries. Copper is a heavy metal, and its soluble salt CuCl$_2$, which is produced in the cell reactions, is a toxic compound. It is especially harmful to aquatic life in lakes, rivers and streams. The Mg/MnO$_2$ battery contains no copper, and MnO$_2$ is known as a non-toxic, water-insoluble compound. Besides the impact on the environment, this difference in toxicity might also impact the occupational health of users and producers of the batteries [4].

4. Conclusions

Manganese dioxide is very suitable for use as a cathode material in water-activated batteries. It is non-toxic, practically insoluble, cheap and light-weight. Its combination with a magnesium anode, the Mg/MnO$_2$ battery, gives a slightly lower voltage than the traditional Mg/CuCl battery, but its voltage is more stable.

In the Mg/MnO$_2$ battery, there is a clear difference between the behaviour of cathode and anode. The manganese dioxide cathode behaves almost ideally at room temperature, and even under low temperature only a moderate overpotential is detectable. The magnesium anode shows strong nonideality and causes high voltage losses, but at the same time it produces the heat needed for battery use in a cold environment. An outside temperature of −60 °C, which is typical of radiosonde use, is not a major problem as the heat evolution keeps the battery temperature above 0 °C. Most aqueous batteries, such as the commercial alkaline battery, congeal at temperatures lower than −20 °C, as they produce only a fraction of this heat.

The water-activated Mg/MnO$_2$ battery can be used for the same applications as the Mg/CuCl battery and

can be seen as its environmentally friendly alternative. The battery has been patented [15].

Acknowledgements

References

1. D.J. Doan, Water-Activated Batteries, *in* N.C. Cahoon and G.W. Heise (Eds), 'The Primary Battery', vol. 2 (John Wiley & Sons, New York, 1976) pp. 295–319.
2. V.S. Bagotsky and A.M. Skundin, 'Chemical Power Sources' (Academic Press, Bury St Edmunds, 1980).
3. H.N. Honer, *US Patent 3 205 096*. Appl.: 28 Dec. (1961), Acc. 7 Sep. (1965).
4. Swiss Toxicity Classification, in the annual Fluka catalogue (1999/2000), Fluka Chemie AG (1999), p. 1609.
5. N.T. Wilburn, 'Magnesium perchlorate reserve battery', Proceedings of the 21st Annual Power Sources Conference, US Army Electronics command, 16–18 May (1967), pp. 113–116.
6. K. Kordesch (Ed.), 'Batteries, Volume 1, Manganese Dioxide' (Marcel Dekker, New York, 1974).
7. A. Moussard, J. Brenet, F. Jolas, M. Pourbaix and J. van Muylder, Manganese, *in* M. Pourbaix (Ed.), 'Atlas of Electrochemical Equilibria in Aqueous Solutions' (NACE, Houston, 1974), pp. 286–293.
8. 'HSC-Chemistry for Windows', version 4.7, Outokumpu Research Oy (1999).
9. M. Hiroi, *J. Appl. Electrochem.* **16** (1986) 431.
10. H.E. Boyer and T.L. Gall (Eds), 'Metals Handbook Desk Edition' (ASM International, OH, 1985), pp. 812–815.
11. K. Vuorilehto and H. Rajantie, *J. Appl. Electrochem.* **29** (1999) 903.
12. D.R. Lide (Ed.), 'CRC Handbook of Chemistry and Physics', (CRC Press LLC, 79th edn, 1998).
13. H. Kantanen, 'Cathode for a Water-Activated Battery', MSc thesis, Helsinki University of Technology, Helsinki (1998).
14. D. Linden (Ed.), 'Handbook of Batteries' (McGraw-Hill, New York, 1995), 2nd edn, p. 7.3–7.22.
15. K. Vuorilehto, *Finnish Pat. Application* FI20 012 040, Appl. 19 Oct. (2001).